This article has been accepted for publication in a future issue of this journal, but has not been fully edited. Content may change prior to final publication. Citation information: DOI 10.1109/JPHOT.2021.3081060, IEEE Photonics Journal

Quantum Dot Coherent Comb Laser Source for Converged Optical-Wireless Access Networks

Haipeng Zhang, Mu Xu, Zhensheng Jia, and Luis Alberto Campos

Cable Television Laboratories Inc., 858 Coal Creek Circle, Louisville, CO 80027, USA

Zhenguo Lu, Chun-Ying Song, Pedro Barrios, Mohamed Rahim, Ping Zhao, and Philip J. Poole

Advanced Electronics and Photonics Research Centre, National Research Council, Ottawa, ON, Canada

Abstract: We propose and experimentally demonstrate a converged optical-wireless WDM access network architecture enabled by a highly integrated quantum dot coherent comb laser. The converged optical-wireless WDM network features simultaneous delivery of coherent and millimeter wave (mmWave) / citizens broadband radio service (CBRS) signals over 50-km and 20km fiber links, respectively.

Index Terms: Fiber optics communications, coherent communications, semiconductor lasers, radio-over-fiber.

1. Introduction

The everlasting growth in data intensive applications and services such as high-definition video-on-demand, cloud computing/storage, Internet of Things, and Big Data, has resulted in continuously increasing in the overall traffic volume in today's communication networks over the last decade. To meet the ever-growing demands for future broadband services, the convergence of fiber-optic and wireless systems has gained widespread interest as one of the most promising solutions to increase the capacity and mobility of the communication systems as well as decreasing the deployment costs in next-generation access networks and mobile xHaul [1-3]. Combining the strength and benefits of high-speed fiber-optic and ubiquitous wireless access technologies, future converged optical-wireless access networks provide a promising solution to support high data-rate, high flexibility, and low latency services [3 - 5].

On the wired optical fiber system side, coherent optics has gradually moved to the edge/access networks due to its superiority in terms of higher data rate, significantly improved receiver sensitivity, and higher spectral efficiency. Furthermore, by utilizing the multi-level advanced modulation formats and digital signal processing, coherent optics effectively compensate linear transmission impairments such as chromatic dispersion (CD) and polarization mode dispersion (PMD), and efficiently utilize the spectral resources [6]. On the other hand, 5G broadband access technologies including millimeter wave (mmWave) and massive internet of things (IoT) offer tremendous benefits in terms of throughput, mobility, and flexibility. Different 5G xHaul solutions have been studied and among them, radio-over-fiber (RoF) technology, which is considered a low-cost and scalable solution, has gain popularity in multi-service broadband access networks [1, 2]. In an RoF system, allocation and control of multiple wireless services takes place in the central office (CO), and ready-to-use analog signals can be delivered to remote access units (RAUs) or base stations (BSs) with identical protocols and interfaces, and thus greatly simplified the cell sites and reduced their cost [2]. Especially, the 5G mmWave small cell system that features low attenuation and low cost can benefit the most from RoF architectures.

A crucial building block that enables optical-wireless convergence is the optical light source. Previous work on mmWave over fiber [7] and integrated optical/RoF networks [8] relied on a single laser source with limited number of optical carriers. Over the past few years, optical frequency comb sources and their applications as monolithic sources of multiple wavelength channels for wavelength division multiplexing (WDM), RoF, and coherent systems have been studied extensively [9-21]. Among different optical frequency comb technologies, mode-locked laser (MLL) sources are very attractive solutions especially for mmWave RoF communication systems due to suppression of phase noise between correlated optical

tones [22-26]. Passively mode-locked lasers based on saturable absorber [23] or quantum dash gain medium [24, 26] have been used extensively for optical mmWave generation. Recently, semiconductor based coherent comb laser (CCL) sources that employ quantum dots (QDs) as the active gain medium have demonstrated features such as compact size, low cost, large mode spacing, low optical phase and relative intensity noises and high-power performance [27-31]. The QD CCLs show a great potential as the monolithic light sources in the broadband optical communication systems. Compared with optical frequency comb generation technologies such as gain switched comb [11], cascaded electro-optic modulators [12-16], and high nonlinear resonator or nano-waveguide [17-20], QD CCL significantly reduces device complexity, power consumption and footprint, does not require accurate control of the RF bias, and does not require high power pump source. The QD CCL benefits from its unique structure, whose gain medium is composed of millions of semiconductor quantum dots with a typical size of less than 50 nm. Each of the quantum dots can function as an independent light source and emit light at its own wavelength. As a result, the QD CCL is a stable multi-wavelength coherent comb source without requiring special mode-locking structures [27-29]. The control of the QD CCL is very simple which only requires a DC bias. Monolithic QD CCL has gained significant interest and is considered to be a very suitable solution to replace many discrete laser devices in high-speed optical communication systems, due to its precisely controlled frequency and channel spacing, as well as low integrated average relative intensity noise [31].

In this work, a converged optical-wireless WDM access network architecture that utilizes a QD CCL is proposed and demonstrated over both fiber and air. The network features simultaneous delivery of wired and wireless signals. The wired connection features 32-GBd dual polarization (DP)-quadrature phase shift keying (QPSK) coherent signal generation and detection over 50-km single mode fiber (SMF) link. The RoF based wireless services include optical mmWave generation and detection, and citizens broadband radio service (CBRS) signal generation and detection through 20 km SMF link. The proposed system significantly reduces the number of light sources by adopting a monolithic QD CCL, offering potential wavelength to end-point services and significant cost and power savings in an access environment where the power budget and operation expenditure (OPEX) are much more stringent compared to long-haul and metro. To support flexible wireless services with various carrier frequencies, future efforts can be made from the following directions. First is to reduce the channel spacing of the QD CCL from 25-GHz to e.g., 6.25 GHz, which can be selectively filtered out by the state-of-art WSS. Then combining with less than 6-GHz intermediate frequency (IF), we will be able to synthesize any frequency beyond 6 GHz. On the other hand, multi-stage cascaded comb source combing the QD CCL with electro-optic modulators [13] or high nonlinear nano-waveguides [20] can also be considered to further broaden the comb spectrum or introduce an extra level of frequency tunability.

2. Quantum Dot Coherent Comb Laser Source

The master light source utilized in this experiment is a monolithic QD CCL, which is an InP-based p-n blocked buried heterostructure (BH) Fabry-Perot (FP) laser with uncoated facets. The laser structure is comprised of a 170 nm thick InGaAsP waveguide core with 10 nm In0.816Ga0.184As0.392P0.608 (1.15Q) barriers embedding five stacked layers of InAs QDs as the active gain region surrounded by n- and p- type InP cladding layers. Chemical beam epitaxy (CBE) was used to grow the InAs QD material on exactly (001)-oriented n-type InP substrates in a similar manner to that in [29]. A detailed schematic for a single dot layer is shown in Fig. 1(a). The 1692 μm long laser waveguide was fabricated via standard photolithography in combination of dry-, wet-etching and contact metallization techniques. After growing the laser core, a 2 μm wide waveguide mesa was created by etching through the 1.15Q waveguide core followed by selective area overgrowth (SAG) of a pnp blocking layer structure that serves to confine carriers to the waveguide mesa. The final p-type InP cladding and contact layers were grown after removing the dielectric mask used for the SAG.

This article has been accepted for publication in a future issue of this journal, but has not been fully edited. Content may change prior to final publication. Citation information: DOI 10.1109/JPHOT.2021.3081060, IEEE Photonics Journal

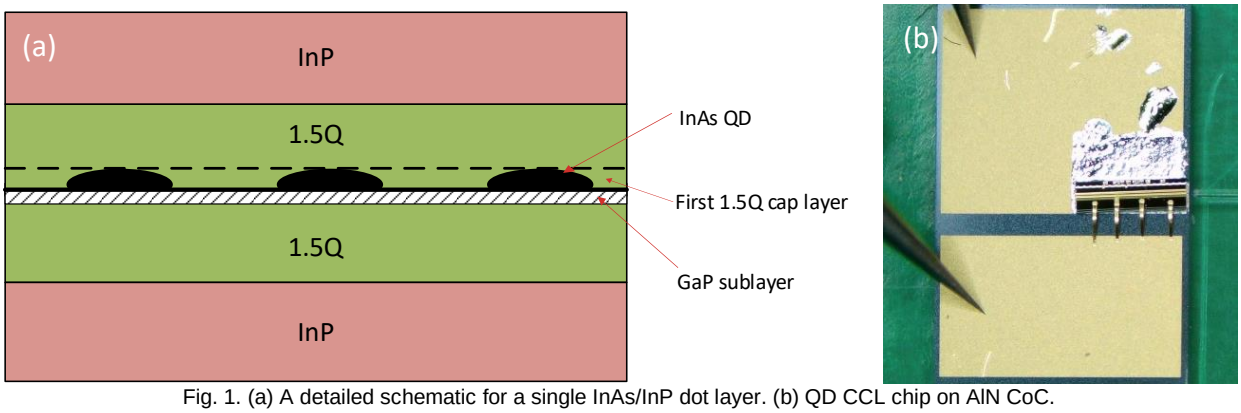

Fig. 1. (a) A detailed schematic for a single InAs/InP dot layer. (b) QD CCL chip on AlN CoC.

The QD laser chip was mounted on a commercially available AlN Chip-on-Carrier (CoC) to provide mechanical support. Two Au electroplated contacts on the CoC provided electrical connections. The cathode (bottom contact) of the QD laser chip was bonded with AuSn eutectic to one of the electrodes of the carrier, and its anode (top contact) was connected to the other electrode via wire bonding, Fig. 1(b) shows the laser chip on the CoC. The laser was powered by a DC power supply through a pair of DC probes, the temperature was controlled by a thermoelectric cooler (TEC). All tests were performed at a drive current of 360 mA under a temperature of 20 °C. During the experiments we did not observe significant fluctuations in wavelength and power of the QD CCL. However, this setup would be insufficient for real world applications, where a laser module with actively stabilized absolute wavelength, power, and channel spacing is needed, like the one reported in reference [30]. The laser output was coupled into a polarization maintaining lensed fiber. A typical optical spectrum of the QD CCL is shown in Fig. 2, with its center wavelength around 1534 nm and 25 GHz frequency spacing between adjacent comb tones. Note that for the current version of the QD CCL chip, part of the optical spectrum is outside the C-band. For the next round fabrication, the optical spectrum could be shifted toward longer wavelength side to ensure all comb tones fall into C-band by optimizing the gain medium material growth.

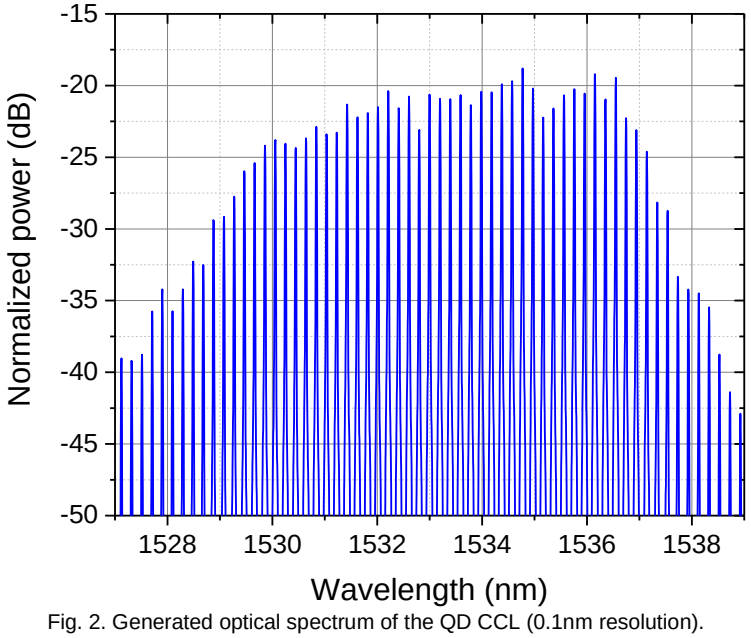

Fig. 2. Generated optical spectrum of the QD CCL (0.1nm resolution).

3. Experimental Setup

The optical-wireless WDM access network link schematic is shown in Fig. 3. In the CO, the optical frequency comb generated by the QD CCL is first amplified by an erbium doped fiber amplifier (EDFA), then separated into multiple tones via a wavelength selective switch (WSS). In the top branch of Fig. 3,

This article has been accepted for publication in a future issue of this journal, but has not been fully edited. Content may change prior to final publication. Citation information: DOI 10.1109/JPHOT.2021.3081060, IEEE Photonics Journal

one of the optical tones is utilized as the optical carrier for coherent signal generation, through a coherent driver modulator (CDM). The coherent signal is a standard 32-GBd DP-QPSK generated with offline code. The DP-QPSK signal is then sent downlink through the 50 km SMF link. At the Endpoint, the optical signal is mixed with a local oscillator (LO) at the same wavelength and detected by an integrated coherent receiver (ICR). The obtained radio frequency (RF) signals for the In-phase and Quadrature (I/Q) components are sent into an optical modulation analyzer acquired at 80GS/s and processed offline with a MATLAB program. The offline coherent DSP code in MATLAB consists of signal resampling and orthogonalization, chromatic dispersion compensation, clock recovery, polarization demultiplex and equalization, carrier frequency offset compensation, and carrier phase recovery. In the middle branch of Fig. 3, another two adjacent optical tones from the QD CCL with 25 GHz spacing are filtered out by the WSS and utilized to generate the mmWave signal. The mmWave signal is a 20 MHz 16-quadrature amplitude modulation (QAM) baseband signal carried 40-MHz intermediate frequency (IF), with a carrier frequency of 25 GHz. Limited by current available hardware in our lab, we use 20 MHz bandwidth which is a standard bandwidth for LTE and CBRS signal, future work will demonstrate higher bandwidth modulation with upgraded hardware. The bias of the Mach-Zehnder modulator (MZM) is set to be Vpi/2. Note that we modulated the real-valued IF signal on two tones simultaneously. After OE conversion through PD, the real-valued IF signal will be beat on to 25-GHz MMW. The operation principle is similar to modulating the two optical tones obtained by optical central carrier suppression (OCS) in reference [1]. We can also modulate the IF signal on one of the two tones. Comparing two-tone co-modulation and single-tone modulation, since the IF signal is real-valued, there will be no significant difference except that the IF signal amplitude after beating would be 3-dB smaller if single-tone modulation is used. Another reason that we used two-tone co-modulation is that in this circumstance we only need to filter two-optical carriers together with a WSS resolution of 25 GHz. If we use single-tone modulation, the WSS resolution must be set to be smaller than 12.5GHz, which will introduce much larger filtering loss and affect the sharpness of the edge of the filtering channel. After 20 km SMF link, at the mmWave BS a high-speed photodiode (PD) with 70 GHz typical bandwidth, flat frequency response and high responsivity is used to convert the optical signal to 25 GHz mmWave, and then sent down link with a horn antenna. On the user equipment (UE) side, the mmWave signal is received by another horn antenna around 2 m away (limited by available lab space) and detected by an envelope detector (ED) that was connected to a vector signal analyzer (VSA). In the bottom branch of Fig. 3, a third optical tone from the QD CCL is utilized to generate the CBRS signal. The single tone is modulated by a Mach-Zehnder modulator (MZM) with electrical up-conversion at 3.5 GHz. A CBRS signal with a baseband of 20MHz 64QAM and a carrier frequency of 3.5 GHz is generated and transmitted over fiber. After 20 km SMF link, at the CBRS BS a high-speed planar PID PD with high sensitivity and support up to 10 Gbits/s data rate is used to convert the optical signal to CBRS signal, and then sent down link with an omnidirectional antenna. On the UE side (~2 m away from the BS), the CBRS signal is detected by a mount style antenna that was connected to another VSA.

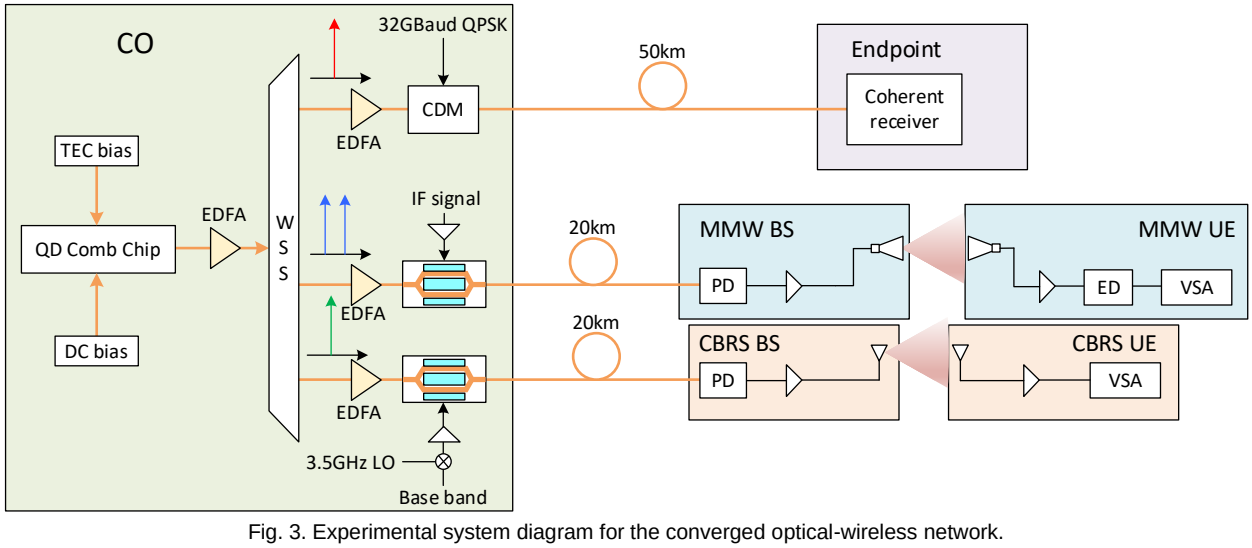

Fig. 3. Experimental system diagram for the converged optical-wireless network.

This article has been accepted for publication in a future issue of this journal, but has not been fully edited. Content may change prior to final publication. Citation information: DOI 10.1109/JPHOT.2021.3081060, IEEE Photonics Journal

The optical spectrum of the optical tones filtered by the WSS are shown in Fig. 4. For wired coherent signal generation, the wavelength of the tone is 1535.695 nm (black curve in Fig. 4). The optical spectrum of the two optical tones for the mmWave generation centered at 1535.28 nm and 1535.472 nm is plotted in red in Fig. 4. Another optical tone for the CBRS signal generation centered at 1535.611 nm is plotted in blue. From the optical spectrum shown in Fig. 4, the adjacent channel isolation of the WSS is greater than 30 dB, which can meet typical requirement for WDM systems (usually >25 dB).

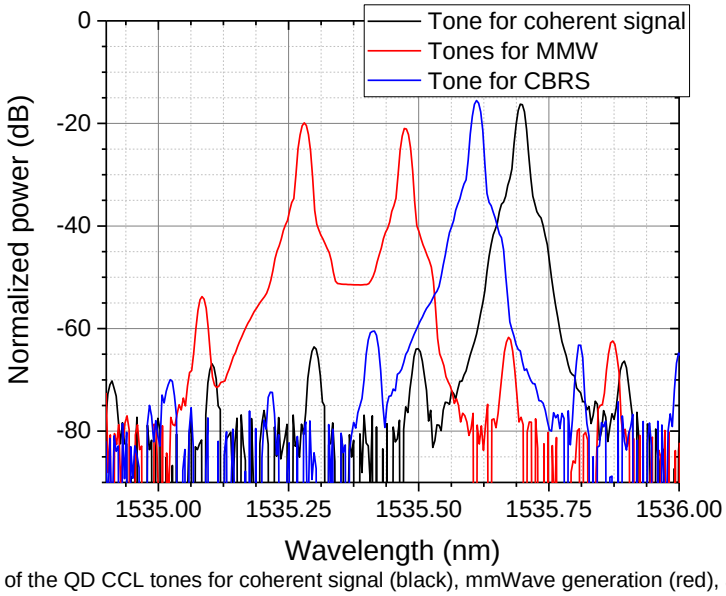

Fig. 4. Optical spectrum of the QD CCL tones for coherent signal (black), mmWave generation (red), and CBRS signal (blue).

4. Results and Discussion

Fig. 5 - 7 show experimental results for the wired and wireless signals generated using the optical tones from the QD CCL. For wired coherent signal generation, the wavelength of the carrier tone is 1535.695 nm, on the receiver side the LO is tuned to match the transmitter wavelength. Over the 50km SMF link, bit error rate (BER) versus received optical power (ROP) for the 32-GBd DP-QPSK coherent signal is plotted in Fig. 5. The staircase hard-decision (HD) forward error correction (FEC) threshold (bit error rate (BER)=4.5E-3) [34] and concatenated soft-decision (SD) FEC threshold (BER=1.2E-2) [35] are included in the plot. The test has been performed using a variable optical attenuator (VOA) to adjust the received optical power at the coherent receiver. For reference purpose, back-to-back (B2B) BER vs. ROP using the same setup is included in the plot. Constellation diagrams for the DP-QPSK signal under -31.33 dBm and -34.33 dBm optical power are included in Fig. 5. The performance of the coherent signal transmission is slightly worse but still comparable with the external cavity laser (ECL)-based system [14, 15], due to a wider linewidth of the optical carrier in the range of a few MHz [27, 29]. Note that the performance of the coherent signal transmission can potentially be further improved by adopting an external cavity self-injection feedback locking system to the QD CCL [27, 29]. For applications in the access network, we would like to keep our laser system simple.

This article has been accepted for publication in a future issue of this journal, but has not been fully edited. Content may change prior to final publication. Citation information: DOI 10.1109/JPHOT.2021.3081060, IEEE Photonics Journal

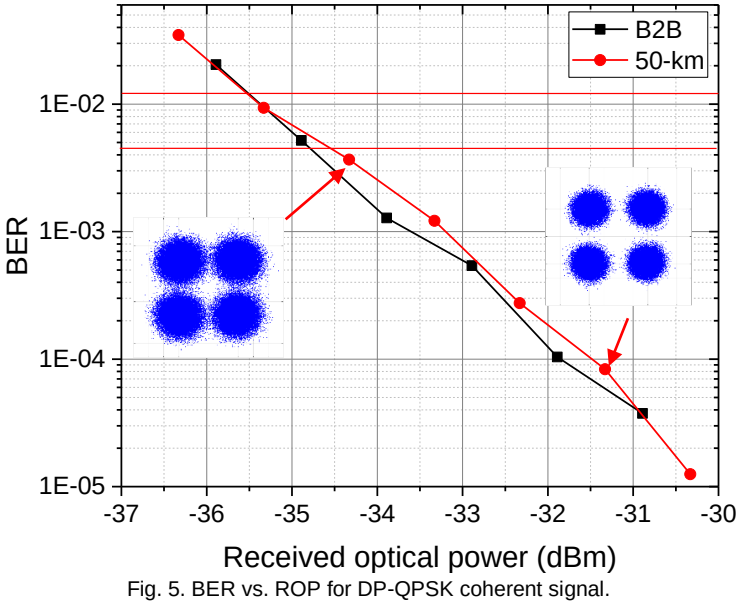

Fig. 5. BER vs. ROP for DP-QPSK coherent signal.

Fig. 6 shows experimental results for the optical mmWave generation using another two of the optical tones (centered at 1535.28 nm and 1535.472 nm) from the QD CCL. Transmitted through the 20km SMF link, error vector magnitude (EVM) vs. ROP for the 20 MHz 16QAM based wireless signal is plotted in Fig. 6. A red line indicating the EVM requirement of 12.5% for 16QAM signal defined by 3rd Generation Partnership Project (3GPP) Long Term Evolution (LTE) technical specification [36] is included in the plot. The ROP is measured at the mmWave BS and adjusted by a VOA, while the EVM is recorded at the mmWave UE. For reference purpose, B2B EVM vs. ROP using the same setup is included in the plot. Compared with the B2B case, around 1 dB penalty is introduced by the 20 km fiber transmission. Constellation diagrams for the 16QAM signal under -11.34 dBm and -23.34 dBm optical power are included in Fig. 6. Since the mmWave generation is based on the optical beating between the two correlated tones from the same comb source, we believe that the phase noise is much suppressed comparing with beating two independent free-running optical carriers. Furthermore, the ED utilized in our experiment helped eradicating the effects of phase noise and frequency offset, as a result we did not observe significant mmWave signal deterioration due to phase noise. If the ED is replaced by a regular heterodyne mmWave receiver with local oscillator [LO], the optical linewidth of the QD CCL tones (on the order of a few MHz [27, 29]) would cause the optical carriers to decorrelate over a relatively short transmission distance. The performance of using a regular mmWave receiver, however, can be further improved by adopting an external cavity self-injection feedback locking system to the QD CCL to reduce the optical linewidth of the optical tones [27, 29].

This article has been accepted for publication in a future issue of this journal, but has not been fully edited. Content may change prior to final publication. Citation information: DOI 10.1109/JPHOT.2021.3081060, IEEE Photonics Journal

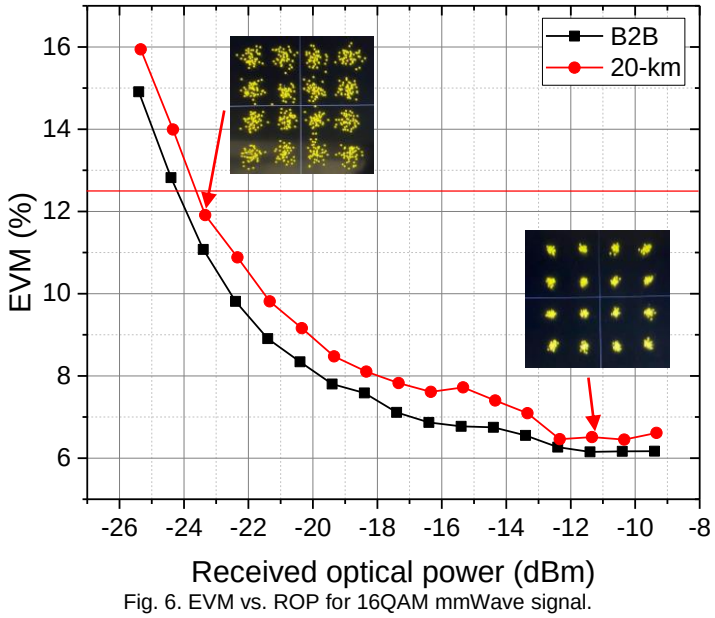

Fig. 6. EVM vs. ROP for 16QAM mmWave signal.

Fig. 7 shows experimental results for the optical CBRS generation using one of the optical tones (centered at 1535.611 nm) from the QD CCL. Transmitted through the 20km SMF link, EVM vs. ROP for the 20 MHz 64QAM based CBRS signal is plotted in Fig. 7. A red line indicating the EVM requirement of 8% for 64QAM signal defined by 3GPP LTE technical specification [36] is included in the plot. The ROP is measured at the CBRS BS and adjusted by a VOA, while the EVM is recorded at the CBRS UE. For reference purpose, B2B EVM vs. ROP using the same setup is included in the plot. Like the mmWave case, around 1 dB penalty is introduced by the 20 km fiber transmission. Constellation diagrams for the 64QAM signal under -10.4 dBm and -18.4 dBm optical power are included in Fig. 7. The optical CBRS generation relies on IM/DD of the optical signal and thus is not strongly affected by the linewidth of the optical carrier. As a result, optical CBRS generation using QD CCL performs comparable the cases of using discrete laser sources.

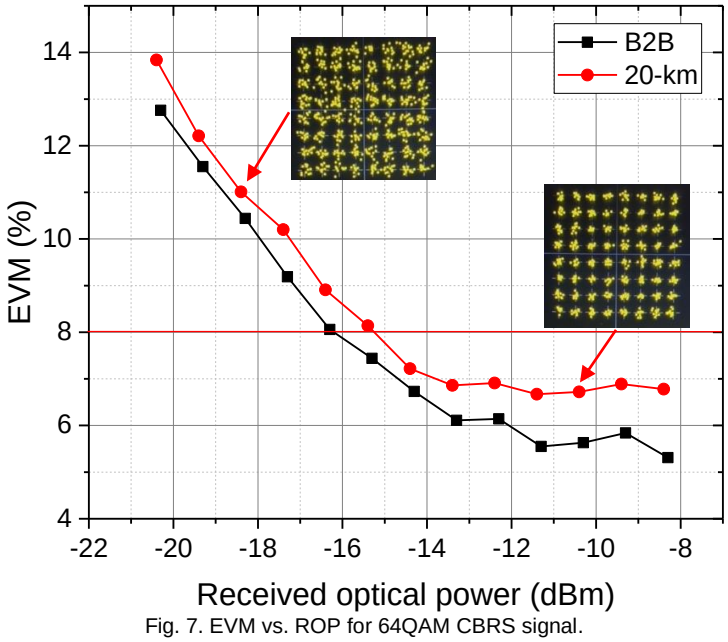

Fig. 7. EVM vs. ROP for 64QAM CBRS signal.

5. Conclusion

We experimentally demonstrated a converged optical-wireless WDM access network architecture,

enabled by a single QD CCL comb laser source, for simultaneous delivery of wired and wireless signals. The wired service features 32-GBd DP-QPSK coherent signal generation and detection over 50 km SMF. The wireless services include optical 25-GHz mmWave generation and detection, and 3.5-GHz CBRS signal generation and detection through 20 km SMF link. Leveraging the highly integrated QD CCL, while maintaining similar system performance, the number of discrete laser sources in this converged optical-wireless WDM access network has been significantly reduced. Generation and control of optical tones remotely from CO facilitate low-cost scalable common platform deployment of future dense wired and wireless networks.

References

[1]. Z. Jia, J. Yu, G. Ellinas, and G. K. Chang, "Key Enabling Technologies for Optical–Wireless Networks: Optical Millimeter-Wave Generation, Wavelength Reuse, and Architecture," J. Lightwave Technol. 25, 3452-3471 (2007).

[2]. M. Zhu, L. Zhang, J. Wang, L. Cheng, C. Liu and G. Chang, "Radio-Over-Fiber Access Architecture for Integrated Broadband Wireless Services," Journal of Lightwave Technology, vol. 31, no. 23, pp. 3614-3620 (2013).

[3]. G. K. Chang and L. Cheng, “The benefits of convergence,” Phil. Trans. R. Soc. A.374: 20140442, (2016).

[4]. P. T. Dat, A. Kanno, N. Yamamoto and T. Kawanishi, "Seamless Convergence of Fiber and Wireless Systems for 5G and Beyond Networks," Journal of Lightwave Technology, vol. 37, no. 2, pp. 592-605, 15 (2019).

[5]. S. E. Alavi, M. R. K. Soltanian, I. S. Amiri, et al, “Towards 5G: A Photonic Based Millimeter Wave Signal Generation for Applying in 5G Access Fronthaul,” Sci Rep 6, 19891 (2016).

[6]. Z. Jia and L. A. Campos, “Coherent Optics for Access Networks,” in CRC Press, ISBN 9780367245764, November 1, 2019.

[7]. Z. Weng, Y. Chi, H. Kao, C. Tsai, H. Wang and G. Lin, "Quasi-Color-Free LD-Based Long-Reach 28-GHz MMWoF with 512-QAM OFDM," Journal of Lightwave Technology, vol. 36, no. 19, pp. 4282-4297, (2018).

[8]. C. Lin et al., "Hybrid Optical Access Network Integrating Fiber-to-the-Home and Radio-Over-Fiber Systems," IEEE Photonics Technology Letters, vol. 19, no. 8, pp. 610-612, (2007).

[9]. Z. Liu, S. Farwell, M. Wale, D. J. Richardson, and R. Slavík, "InP-based Optical Comb-locked Tunable Transmitter," Optical Fiber Communication Conference (2016), paper Tu2K.2.

[10]. V. Torres-Company et al., "Laser Frequency Combs for Coherent Optical Communications," Journal of Lightwave Technology, vol. 37, no. 7, pp. 1663-1670, (2019).

[11]. M. D. G. Pascual, V. Vujicic, J. Braddell, F. Smyth, P. Anandarajah and L. Barry, "Photonic Integrated Gain Switched Optical Frequency Comb for Spectrally Efficient Optical Transmission Systems," IEEE Photonics Journal, vol. 9, no. 3, pp. 1-8, (2017).

[12]. S. Fukushima, C. F. C. Silva, Y. Muramoto, and A. J. Seeds, "Optoelectronic Millimeter-Wave Synthesis Using an Optical Frequency Comb Generator, Optically Injection Locked Lasers, and a Unitraveling-Carrier Photodiode," J. Lightwave Technol. 21, 3043- (2003).

[13]. C. Zhang, T. G. Ning, J. Li, L. Pei, C. Li, and S. Ma, “A full-duplex WDM-RoF system based on tunable optical frequency comb generator,” Optics Communications, Volume 344, pp. 65-70, 2015.

[14]. H. Zhang, M. Xu, J. Zhang, Z. Jia, L. A. Campos and C. Knittle, "Highly Efficient Full-Duplex Coherent Optical System Enabled by Combined Use of Optical Injection Locking and Frequency Comb," Journal of Lightwave Technology, vol. 39, no. 5, pp. 1271-1277, 1 (2021).

[15]. H. Zhang, M. Xu, J. Zhang, Z. Jia, and L. A. Campos, “Full-duplex Coherent Optical System Enabled by Comb-Based Injection Locking Optical Process”, Optical Fiber Communication Conference (2020), paper T4G.4.

[16]. J. Zhang, N. Chi, J. Yu, Y. Shao, J. Zhu, B. Huang, and L. Tao, "Generation of coherent and frequency-lock multi-carriers using cascaded phase modulators and recirculating frequency shifter for Tb/s optical communication," Opt. Express 19, 12891-12902 (2011).

[17]. J. Pfeifle, V. Brasch, M. Lauermann, et al, “Coherent terabit communications with microresonator Kerr frequency combs,” Nature Photon 8, 375–380 (2014).

[18]. P. Marin-Palomo, J. Kemal, M. Karpov, et al, “Microresonator-based solitons for massively parallel coherent optical communications,” Nature 546, 274–279 (2017).

[19]. B. Wang, J. S. Morgan, K. Sun, et al, “Towards high-power, high-coherence, integrated photonic mmWave platform with microcavity solitons,” Light Sci Appl 10, 4 (2021).

[20]. H. Hu, F. Da Ros, M. Pu, et al. “Single-source chip-based frequency comb enabling extreme parallel data transmission,” Nature Photon 12, 469–473 (2018).

[21]. C. Weimann, P. C. Schindler, R. Palmer, S. Wolf, D. Bekele, D. Korn, J. Pfeifle, S. Koeber, R. Schmogrow, L. Alloatti, D. Elder, H. Yu, W. Bogaerts, L. R. Dalton, W. Freude, J. Leuthold, and C. Koos, "Silicon-organic hybrid (SOH) frequency comb sources for terabit/s data transmission," Opt. Express 22, 3629-3637 (2014).

[22]. K. Kitayama, T. Kuri, H. Yokoyama and M. Okuno, "60 GHz millimeter-wave generation and transport using stabilized mode-locked laser diode with optical frequency DEMUX switch," IEEE Global Telecommunications Conference, 1996, pp. 2162-2169 vol.3.

[23]. G. A. Vawter, A. Mar, V. Hietala, J. Zolper and J. Hohimer, "All optical millimeter-wave electrical signal generation using an integrated mode-locked semiconductor ring laser and photodiode," IEEE Photonics Technology Letters, vol. 9, no. 12, pp. 1634-1636, 1997.

[24]. F. van Dijk et al., "Quantum dash mode-locked lasers for millimeter wave signal generation and transmission," 23rd Annual Meeting of the IEEE Photonics Society, 2010, pp. 187-188.

[25]. H. Elwan et al., “Impact of laser mode partition noise on optical heterodyning at millimeter-wave frequencies,” J. Lightw. Tech., 34, 4278-4284, 2016.

[26]. A. Delmade, T. Verolet, C. Browning, Y. Lin, G. Aubin, F. Lelarge, A. Ramdane, and L. P. Barry, "Quantum Dash Passively Mode Locked Laser for Optical Heterodyne Millimeter-Wave Analog Radio-over-Fiber Fronthaul Systems," Optical Fiber Communication Conference 2020, paper W2A.41.

[27]. Z. G. Lu, J. R. Liu, P. J. Poole, C. Y. Song, and S. D. Chang, "Ultra-narrow linewidth quantum dot coherent comb lasers," Optical Fiber Communication Conference (2018), paper Th1I.5.

[28]. Z. G. Lu, "Quantum-dot coherent comb lasers for terabit optical networking systems", Proc. SPIE 10921, Integrated Optics: Devices, Materials, and Technologies XXIII, 109210N (2019).
[29]. Z. G. Lu, J. R. Liu, C. Y. Song, J. Weber, Y. Mao, S. D. Chang, H. P. Ding, P. J. Poole, P. J. Barrios, D. Poitras, S. Janz, and M. O'Sullivan, "High performance InAs/InP quantum dot 34.462-GHz C-band coherent comb laser module," Optics Express, 26, 2160-2167 (2018).
[30]. Z. G. Lu, J. R. Liu, C. Y. Song, J. Weber, Y. Mao, S. D. Chang, H. P. Ding, P. J. Poole, P. J. Barrios, D. Poitras, S. Janz, and M. O'Sullivan, "High performance InAs/InP quantum dot 34.462-GHz C-band coherent comb laser module," Opt. Express 26, 2160-2167 (2018).
[31]. Z. G. Lu, J. R. Liu, P. J. Poole, S. Raymond, P. J. Barrios, D. Poitras, G. Pakulski, P. Grant, and D. Roy-Guay, "An L-band monolithic InAs/InP quantum dot mode-locked laser with femtosecond pulses," Opt. Express, 17, 13609–13614 (2009).
[32]. J. R. Liu, Z. G. Lu, S. Raymond, P. J. Poole, P. J. Barrios, G. Pakulski, D. Poitras, G. Z. Xiao, and X. Y. Zhang, "Uniform 90-channel multiwavelength InAs/InGaAsP quantum dot laser," Electron. Lett., 43, 8, 458-460 (2007).
[33]. P. J. Poole, K. Kaminska, P. J. Barrios, Z. G. Lu and J. R. Liu, "Growth of InAs/InP-based quantum dots for 1.55 μm laser applications," J. Cryst. Growth, 311, 1482–1486 (2009).
[34]. Optical Interworking Forum 400G ZR standard.
[35]. International Telecommunication Union (ITU-T) G.709.2 recommendation.
[36]. 3GPP LTE Technical Specification 36.141 version 12.6.0 Release 12.
[37]. F. Brendel, et al, "Chromatic dispersion in 60 GHz radio-over-fiber networks based on mode-locked lasers," J. Lightwave Technol. 29, 3810–3816 (2011).